Analysis of meso-scale effects in High Shear Granulation through a CFD-PBM coupled compartment model

P.J. Abrahamsson[1], P. Kvist[1], G. Reynolds[2], X. Yu[3], I. Niklasson Björn[4], M. J. Hounslow[5], A. Rasmuson[1*]

1 Department of Chemical and Biological Engineering, Chalmers University of Technology, SE-412 96 Gothenburg, Sweden
2 Pharmaceutical Development, AstraZeneca, Macclesfield, SK10 2NA, UK
3 European Bioenergy Research Institute (EBRI), School of Engineering and Applied Science, Aston University, Birmingham B4 7ET, UK
4 Department of Chemical and Biological Engineering, the University of Sheffield, Sheffield, S1 3JD, UK
5 AstraZeneca Pharmaceutical and Analytical R&D, Mölndal, SE-431 83 Mölndal, Sweden

*Corresponding author, email: rasmuson@chalmers.se

Keywords: High Shear Wet Granulation, Population Balance Model, Compartment Model, CFD

Abstract

In high shear granulation it has been pointed out that there is a need for meso-scale resolution and coupling between flow field information and the evolution of particle properties**.** In this article we develop a modelling framework that compartmentalizes the high shear granulation process based on process relevant parameters both in time and space. It is built up by a coupled flow field and population balance solver and is used to resolve and analyze the effects of meso-scales on the evolution of particle properties. A Diosna high shear mixer is modelled with micro crystalline cellulose powder as the granulation material. The analysis of the flow field solution and compartmentalization allows for a resolution of the stress and collision peak at the impeller blades. Different compartmentalizations were done showing the importance of resolving the impeller region, both for only aggregating systems and systems with breakage. An investigation on the time evolution of the flow field depending on the changing particle properties was also done, indicating the importance of resolving meso scale phenomena in time as well as space.

1. Introduction

In a recent review on high shear granulation modeling [1] it was pointed out the special need for meso-scale resolution and coupling between flow field information and the evolution of particle properties. Also in the granulation review [2] this issue is stressed, pointing at the need for flow pattern analysis

for different types of granulators and how it can be coupled to the mixing behavior and impact velocities of the individual granules. A tool that could solve flow properties for vessels of all types and sizes and relate it to the evolution of particle properties would be of great value for scale up and process control.

Population balance modeling is the main modeling tool for following the evolution of particle properties in a granulation process. The models are often based on the assumption of a well-mixed vessel with experimentally found averaged rate constants for growth and breakage. There is a development towards flow-dependent mechanistic kernels which is pointed out in the recent review by Kumar et.al. [1]. As an example Tan et. al. [3] has demonstrated how a growth kernel can be derived based on the kinetic theory of granular flow. This includes the local random particle motion as a time dependent part next to the more classical size dependent aggregation kernel developed by Hounslow [4]. A mechanistic model for breakage of a wet granule was derived by Ramachandran et al [5] where they in detail account for all forces acting on a granule and compare it to the internal forces holding the aggregate together. Such a comparison of internal and external forces was also applied by Liu et.al [6] where they use a Stokes deformation number to classify the type of aggregation that takes place at a certain collision energy. This type of analysis shows the importance of resolving stress peaks and estimating local collision velocities since one average value will only capture one of the potentially many regimes present with in a vessel. That type of information could be collected either through experiments or simulations. Nilpawar et al [7] has examined aggregation efficiency by experimentally observing surface velocity fluctuations to estimate collision frequencies in order to experimentally obtain kernel information.

The flow field in a granulator has been modeled using two different approaches, the discrete element method, DEM, and continuum modeling of the granular phase. Gant et.al. [8] used DEM simulations to extract collision rates and energies in a disc-impeller granulator to use for PBM kernels. The disadvantage of the DEM method is that it becomes impractical for industrial size granulators where the number of particles may, by orders of magnitude, exceed 10^6. The continuum approach to particle flows in high shear granulation was first used by Darelius et al [9] and Ng et al [10]. This has further been studied by Abrahamsson et al [11-13] and developed by Khalilitehrani et al [14-16] which shows promising results but also a need for further development. The HSG process is a continuously changing system where the continuous changes in particle properties are bound to affect the flow field and vice versa. To locally resolve collision properties at every instance in time would be too computationally expensive even for the use of continuum models. Some discretization (compartmentalization) of the system in both time and space is needed. Abrahamsson et.al. [11] investigated the effects of changing particle properties on the flow field of a disc-impeller granulator to study the time discretization of a

granulation. For the spatial discretization, compartment models have been developed and used within many other chemical engineering applications [17-22]. A theoretical framework [23], as well as an automatic zoning process [24] for hybrid compartmental-CFD modeling were developed by Bezzo et al. Bezzo later applied this framework to a batch bioreactor [17] to account for imperfect mixing with regard to viscosity. Another approach was developed by Iliuta et al [18] using compartments to separate gasification and combustion during an incineration. Guha et al [19] modeled a single phase stirred-tank reactor and discretized the tank based on the characteristic reaction time scale which showed to capture the essential features of macro mixing. In crystallization Kougoulos et al [25] continued the work by Bermingham, Kramer and ten Cate [26-28] by creating compartments with respect to energy dissipation rate, temperature distribution and solid concentration from CFD simulations. Within high shear granulation the well mixed assumption is commonly used. However, the lack of incorporation of flow field and meso-scale information makes the predictability of the models for new types of equipment limited. An attempt to compartmentalize a high shear granulator was done by Xi Yu [29]. With similar heuristics as was used for a crystallizer [26], a simple method of finding compartments for high shear granulation was realized.

In this article we further develop a model framework that can discretize (compartmentalize) the high shear granulation process based on process relevant parameters both in time and space. It is built up by a coupled flow field and population balance solver and is used to resolve and analyze the effects of meso-scales on the evolution of particle properties.

2. Model theory

In this section the different parts of the developed model will be explained. It starts with giving the necessary information on the system that is modeled and thereafter motivating the choice of population balance equation, kernels and solver method. After that the CFD model is described and finally the compartmentalization method developed will be presented and the coupling between the CFD and PBM solver addressed discussing the relevant flow parameters and their relation to the PBM kernels.

2.1 System modeled

The system is based on a laboratory scale DIOSNA high shear granulator with a volume of four liter with a three bladed beveled impeller rotating at 600 rpm, the outlines of the vessel can be seen in Figure 1 where the computational mesh set up is also shown. The properties of the granular material for the CFD Cases is set to mimic those of micro crystalline cellulose granules at different stages of a granulation [11], Table 1.

Table 1. Particle properties in the CFD cases. d is particle average diameter, e is the particle-particle restitution coefficient, phi is the angle of internal friction, B.C. is a measure of the boundary slip.

Case	**1**	**2**	**3**
d	59µm	400µm	800µm
e	0,9	0,9	0,9
phi	35 ^{o}	32,5^{o}	30 ^{o}
B.C	1	10	100
Pack lim.	0,65	0,65	0,65
Density	750Kg/m^3	750Kg/m^3	750Kg/m^3

Variations in the properties were then made in order to mimic the changes in particle properties as the granulation progresses. This was done in accordance to [11] where the CFD cases are set up to mimic the evolution of the properties stated.

2.2 Population balance modeling

A two dimensional population balance equation, for solid and liquid mass, was used and can be seen in equation 1. The choice of a two dimensional PBM was made as a first trial for the compartment framework. We believe that a higher dimensionality and complexity of the mechanisms would lead to a more non-uniform system and more elaborate criteria for the compartmentalization. It is solved by a constant volume Monte Carlo method developed and validated by Xi Yu [29].

$$\frac{V_i \partial n_i(m_s,m_l,t)}{\partial t} = V_i B_0^0 B(m_s,m_l) + V_i R_w^0 R_w(m_s,m_l) + V_i G_0 \frac{\partial n_i(m_s,m_l,t) G(m_s,m_l,t)}{\partial m_s} + \frac{1}{2} V_i \beta_0 \int_0^{m_s} \int_0^{m_l} \beta(m_s,m_l,m'_s,m'_l)\, n_i(m_s - m'_s, m_l - m'_l, t) n_i(m'_s,m'_l,t) dm_s dm_l - V_i \beta_0 n(m_s,m_l,t) \int_0^{\infty} \int_0^{\infty} \beta(m_s,m_l,m'_s,m'_l)\, n_i(m'_s,m'_l,t) dm'_s dm'_l + \sum_{j=1,j\neq i}^{k} \frac{Q_{i\to j}}{V_i} n_i(m_s,m_l,t) + \sum_{j=1,j\neq i}^{k} \frac{Q_{j\to i}}{V_j} n_j(m_s,m_l,t) \quad (1)$$

where $\boldsymbol{m_s}, \boldsymbol{m_l}$ are the mass in kg of solid and liquid respectively in the granule, V is the compartment volume in $m^3$and Q is flow rate to and from compartments in $\frac{\boldsymbol{m^3}}{\boldsymbol{s}}$. n is the density function, $\frac{\boldsymbol{number\ of\ particles}}{\boldsymbol{kg^2 m^3}}$. G, B, R and β are layering, nucleation, rewetting and aggregation respectively, which are the mechanisms used.

In this paper the aggregation kernel by Tan et al [3] will be used. The derivation of the aggregation kernel [3] is based on the principles of kinetic theory of granular flow (KTGF) and the equi-partition of kinetic energy (EKE) kernel developed by Hounslow [4]**.** The aggregation kernel can be seen in equation 2 below

$$\beta_{i,j} = \psi g_{i,j} \sqrt{\frac{3\theta_s}{\rho}} (l_i + l_j)^2 \sqrt{\frac{1}{l_i^3} + \frac{1}{l_j^3}} \quad (2)$$

where ψ is the aggregation efficiency, θ_s is the mixture granular temperature which is similar to the description of granular temperature in KTGF, equation 3.

$$\theta_s = \frac{1}{3} m_n \langle C \cdot C \rangle = m_n \theta \quad (3)$$

where m_n is the average mass of a particle and C is the random fluctuating part of the decomposed actual particle velocity from the KTGF. The aggregation kernel consists of one size dependent part, which is the EKE kernel, equation 4.

$$\beta(l_i, l_j) = (l_i + l_j)^2 \sqrt{\frac{1}{l_i^3} + \frac{1}{l_j^3}} \quad (4)$$

and a time dependent part, equation 5.

$$\beta_0(t) = \psi g_0 \sqrt{\frac{3\theta_s}{\rho}} \quad (5)$$

where l is particle size, g_0 the radial distribution function of particle volume fraction defined as seen in equation 6.

$$g_0 = \left[1 - \left(\frac{\alpha_s}{\alpha_{s,max}}\right)^{1/3}\right]^{-1} \quad (6)$$

Of special interest is the time dependent part of the aggregation kernel, equation 5, which will be calculated from CFD simulations rather than found experimentally. Benefits from actually calculating this is not only that no experiments for the specific granulator are needed, but it is also a way to estimate the actual rate of aggregation locally in the system.

The layering mechanism used is that developed in [30]. The nucleation and rewetting rates are dependent on the liquid binder addition. The liquid binder is added in a special compartment and the initial drop addition rate is described in equation 7.

$$r_d = \frac{v\dot{M}_{drop}}{\overline{m}_{drop}} \quad (7)$$

where $\dot{M}_{drop}$ is the spray rate in kg/s, $\overline{m}_{drop}$ is the mean mass of droplets in the simulation and v is the volume sample size. Both spray rate and the mean drop size can be determined from experiments and be adjusted depending of what type of spray is present.

The probability of a droplet either re-wetting an existing granule or creating a nucleus by contact with primary particles can be assumed to be proportional to the projected surface area of each population, according to equations 8 and 9.

$$b_0 = \frac{A_p}{A_p + A_g} r_d \quad (8)$$

$$r_w = \frac{A_g}{A_p + A_g} r_d \quad (9)$$

where b_0 is the nucleation rate and r_w is the re-wetting rate. Subscripts p and g are particle and granule respectively with A being the projected area of each population.

Breakage is described by the volume dependent breakage function with uniform fragment distribution that is used and described in Hounslow et.al. 2001 [31]. This simple empirical function does not give a direct connection to the flow conditions in the vessel, however here we will use a breakage rate that is affected by the local flow conditions. The breakage rate is related to the forces acting on the granules and the internal strength of the aggregates. Since the equations do not contain any dimension of compaction or change in mechanical properties, the internal strength cannot be estimated here. The external forces are related to the flow conditions and especially the collision velocities between granules and between granules and the vessel [6]. The collision velocities are assumed to be proportional to the granular temperature and the shear rate in the vessel.

2.3 The CFD model

CFD simulations have been carried out in Ansys Fluent 13 and the details are reported in Xi Yu [29]. The lower part of the geometry is the rotating region, in which the impeller is rotated by a sliding mesh technique, the mesh is visualized in figure 1.

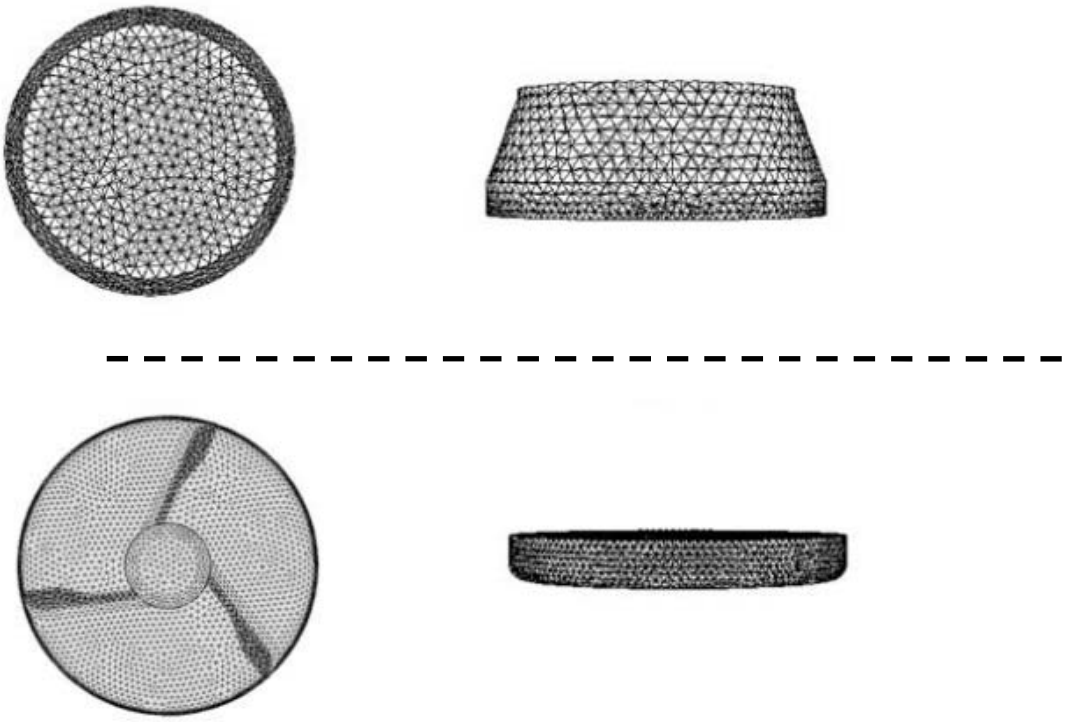

Figure 1. Side and top view of the two regions in the granulator. Above the dashed line is the static part and below is the rotating part.

The modeling of the particle phase continuum properties were made with the kinetic theory of granular flow with added frictional stress in the dense regions, based on the work by Darelius et.al.[9] and Ng et.al. [10]. These models have shown to be able to predict the main features of the particle flow in a HSG. There are deficiencies in the detailed flow predictions [12]. However, in this work a new modeling framework is developed and the method it is not dependent on the specific choice of flow model. More accurate models for dense granular flows are needed and under development [13-16] for more reliable results. The present modeling framework is, however, not affected by the detailed flow modeling and in future work more accurate flow simulations can easily be incorporated.

For details on the model equations the model setup is equivalent to that used in Darelius et.al [9] and Abrahamsson et.al. [11] but with the particle properties presented in table 1.

2.4 Meso scale analysis and Compartment model

The meso-scale analysis is based on the analysis of mass distributions of a set of important properties required for the PBM solver, discussed further down in this section, together with a spatial analysis of where regions of different values are found. The regions are then merged into compartments with

similar kernel information for the PBM solver. The inter-compartmental fluxes are also extracted and used in the PBM solver.

The compartment model analysis was made by extracting cell data from FLUENT for examination in MATLAB (MathWorks, R2012b). The general method used follows a separation of cells based on a sorting mechanism, by starting from the highest value in the system with regard to granular temperature for example, and finding all similar values within a set interval. The interval can be set using a tolerance $\tau < 1$ such that $Find(P) = Max(P) * \tau$, where P is any property of interest in the system. Coordinates in space are extracted along with the value and if cell values are adjacent to each other a compartment can be defined. The algorithm is semi-automatic and requires inspection to find appropriate values for continuous compartments to form.

Properties that are important for the granulation process include volume fraction and granular temperature. Both of these are critical for how growth of granules evolve over time. Furthermore the time dependent part of the aggregation kernel, β_0, is a function of both volume fraction and granular temperature and will be used as the critical parameter of choice to determine compartments. The local strain rates will also be analyzed together with the granular temperature to give an indication on the relative breakage rates in different regions of the vessel. Collection of volumes, solid volume fraction, β_0 and interconnected flow rates for all compartments are performed by a user defined function (UDF) in Fluent. This is done over a time period of 1 second (10 impeller revolutions) to account for variations in the system.

The compartment locations, internal properties and connecting fluxes are given from the CFD solution to the PBM solver. The particle properties change in the PBM and the new properties can be used to update the CFD solution. Figure 2 shows a flow sheet of the developed CFD . PBM compartment model. In this work the PBM solution is not used to update the CFD model due to the simple PBM model used. Instead literature data particle properties are used to get the effect of particle property changes as the granulation progresses, the properties for the CFD cases are described in table 1.

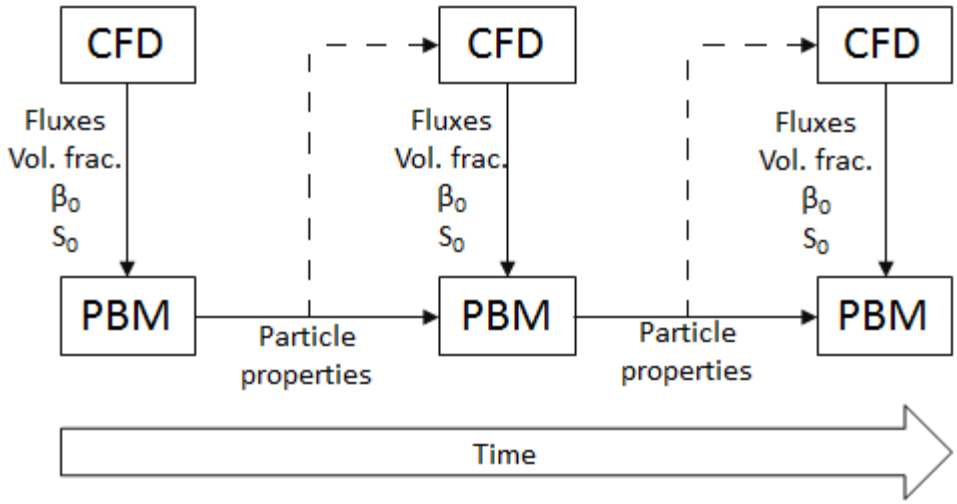

Figure 2. The flow sheet of the CFD – PBM compartment model.

3. Results and discussion

The results will be divided and discussed by first a general analysis of the CFD solution, analyzing the different distinguishable regions found in the vessel. After this the results of the spatial compartment model will be discussed and finally the results of the temporal resolution are analyzed. The flow field and compartment will be analyzed, in detail, for one CFD case only. The temporal analysis is made for all CFD cases.

3.1 General flow field analysis

The flow pattern in all the CFD simulations shows a roping torus with a large void in the center, as seen in Figure 3 for CFD-case 2 (c.f. Table 1). In the lower part of the bowl, there are dense regions at the impeller blades followed by more dilute tails extending to the next blade. This agrees in general with experimental observations and is the same for all cases.

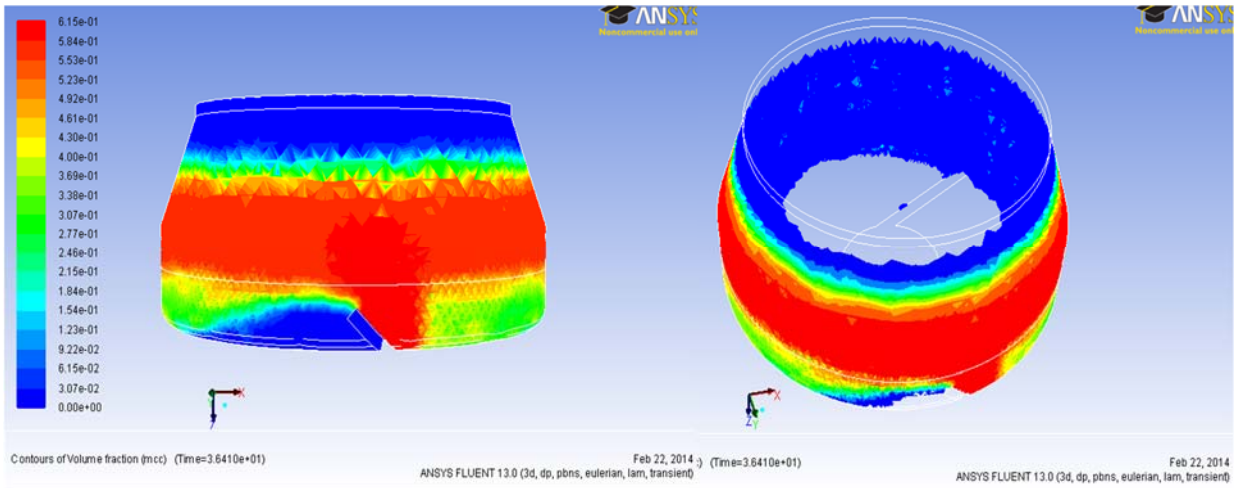

Figure 3. Two different views of volume fraction larger than 0.01 plotted as contours.

The cell data was analyzed in Matlab in order to sort out regions of different behaviors in the vessel. Figure 4 shows the distribution of aggregation rate values and the geometrical location of the particles (in mass) with the 10% highest values.

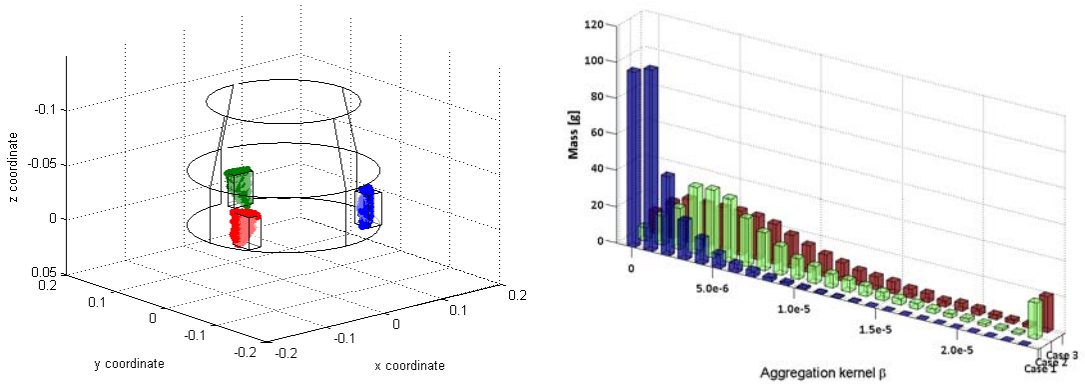

Figure 4. Impeller compartments separated based on β_0. Coordinate axis are distance in meters.

This shows that there are clearly different regions in the granulator in terms of aggregation where the high value peak (seen for case 2 and 3) is shown in the vessel outline to be located on the impeller blade tips. The spatial analysis also shows a tail of intermediate aggregation rate in the lower volume fraction region between the impeller blades, while the upper region has in general much lower values and shows a radial distribution of the aggregation rate with values decreasing towards the walls. The exact analysis is of lesser importance since the accuracy of the flow model is limited but this shows the potential of the model and the analysis capabilities of the framework.

Based on this several compartmentalisation cases were constructed, the outline of the compartment cases can be seen in Table 2 and figure 5. Compartment 1 is a spray compartment which is where the binder liquid is added. Its layout is based on Xi Yu's [29] assumptions, calculations and experimental values that are assumed to apply for a common spray found in high shear granulation equipment. There is also a natural compartment division in the separation in the mesh between the rotating bottom part and the stationary upper part which has been taken into consideration.

Table 2. General information on the four constructed compartment cases

	Number of compartments	Comment
Comp. 1	2	Whole granular volume as one compartment.

Comp. 2	2	Void in center removed, still one compartment.
Comp. 3	3	Geometrical separation of static and rotating part.
Comp. 4	4	Adding the impeller compartment.

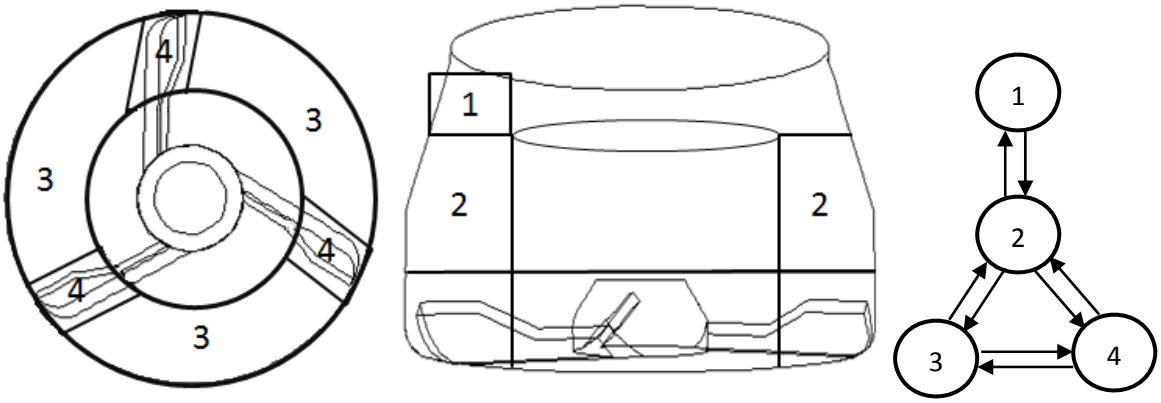

Figure 5. The compartments of the granulator and their connection scheme to the right.

The compartment division and values will be presented in detail for the case Comp. 4, the values for the other compartment cases can be found in Appendix 1. The volumes, solid volume fractions and aggregation rate values for the different compartments can be found in Table 3. The values given are averages over the compartments. All values are based on a one second time average, which represents the average of ten impeller revolutions.

Table 3. The properties inside the different compartments in CFD-case 2 and compartmentalization Comp. 4.

CFD-case 2 and compartmentalization Comp. 4

Compartment	Volume [m^3]	Volume fraction solid	β_0 [m/s]	S_0 [s^{-1}]
1	2,0e-05	0,30	0	0
2	1,0e-03	0,34	5,0e-06	0,04e7
3	4,8e-04	0,08	2,7e-06	0,40e7
4	8,1e-05	0,28	1,9e-05	0,80e7

In addition to the properties of each compartment, the volume flow rates of solids between the compartments are also extracted, Table 4. The total volume of solids in the vessel is 4e-4m^3 and this

shows that the flow between the compartments is high. The residence time in the large second compartment is for example in average about 1s.

Table 4. The inter-compartmental fluxes for the CFD-case 2 and compartmentalization Comp. 4.

Flow rates from CFD-case 2 and compartmentalization Comp. 4 [m3/s]				
Compartment	**1**	**2**	**3**	**4**
1	0	7,5e-03	0	0
2	7,5e-03	0	6,3e-04	3,9e-04
3	0	5,6e-04	0	0
4	0	7,8e-05	2,1e-03	0

A first trial of the model was made without breakage using aggregation rates as the factor for dividing the compartments and providing compartment volumes, solid volume fractions, aggregation rates and inter-compartmental solid flow rates to the PBM. All compartment cases were treated to investigate the effect of the compartmentalization. Figure 6 shows the resulting particle size distribution after 5min of granulation. The results show that the compartmentalization does effect the solution even with the same solid volume weighted average of the aggregation and no breakage. The error bars are due to the stochastic Monte Carlo solver which does give some spread in the results. The results are based on ten replications with 5000 particles, and was found to give a stable representative average. There is no clear trend that more compartments pushes the final particle size distribution in any defined direction. However, the use of an impeller compartment (Comp. 4) gives a significantly higher aggregation rate demonstrating the importance of identifying regions with high activity.

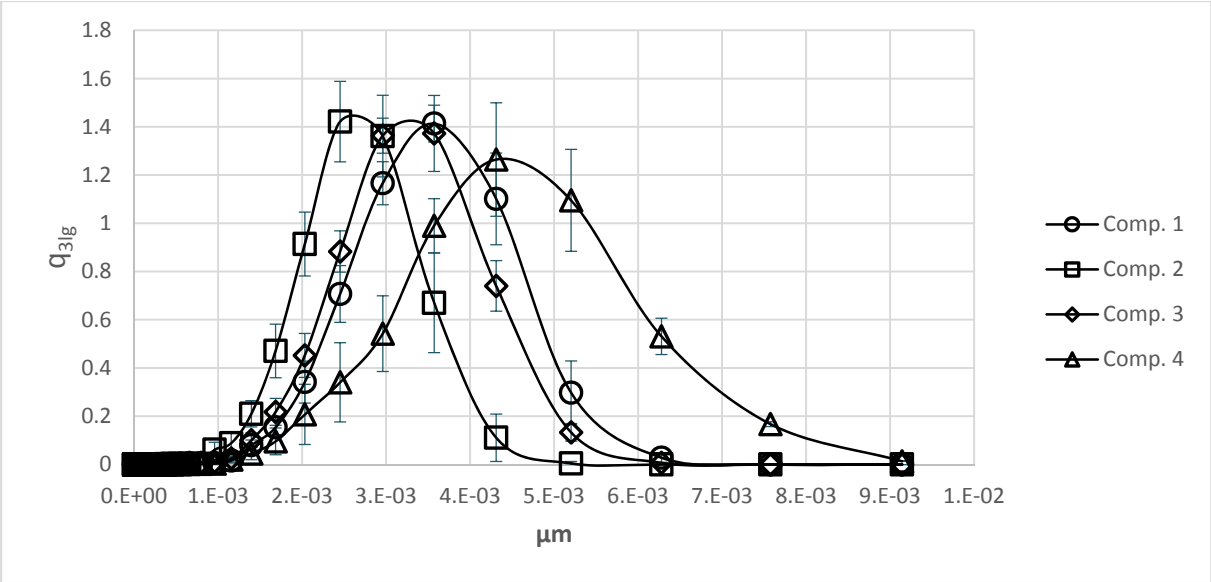

Figure 6. Granulation size distribution for the four compartmentalization's after 5 minutes.

The results show that despite the rapid mixing and that the aggregation rate is linearly related to the evolution of the particle diameter one average value cannot represent the process well, and a spatially resolved aggregation rate does affect the solution. The information of the geometric regions with different aggregation rates is of importance for the design of the equipment. The system used is a lab scale equipment, in a production scale equipment the mixing and the inter-compartmental fluxes are bound to decrease. This would lead to presumably even bigger impact of the compartmentalization and a less well mixed system. The possibility to compare large scale and small scale simulations would also lead to an improved understanding of scale up effects.

For breakage the shear rate and collision energies are the important factors. An analysis of the granular temperature and local shear rate was made to determine the relation between the compartment values. The Figures 9 and 10 show the mass-distribution of granular temperature and strain rate for three CFD cases. A geometrical analysis shows that the high regions of strain and granular temperature coincide in front of the impellers. Since we lack information on the granular strength properties, threshold values for when breakage occurs cannot be calculated. The values of the breakage rates were set according to Table 3. The size range of the values were chosen in order to have an effect of the breakage over the time simulated. The individual compartment values where set based on the idea of a small average stress in the whole vessel, with a stress peak by the impeller. Figure 7 shows the final particle size distributions after five minutes of calculated granulation

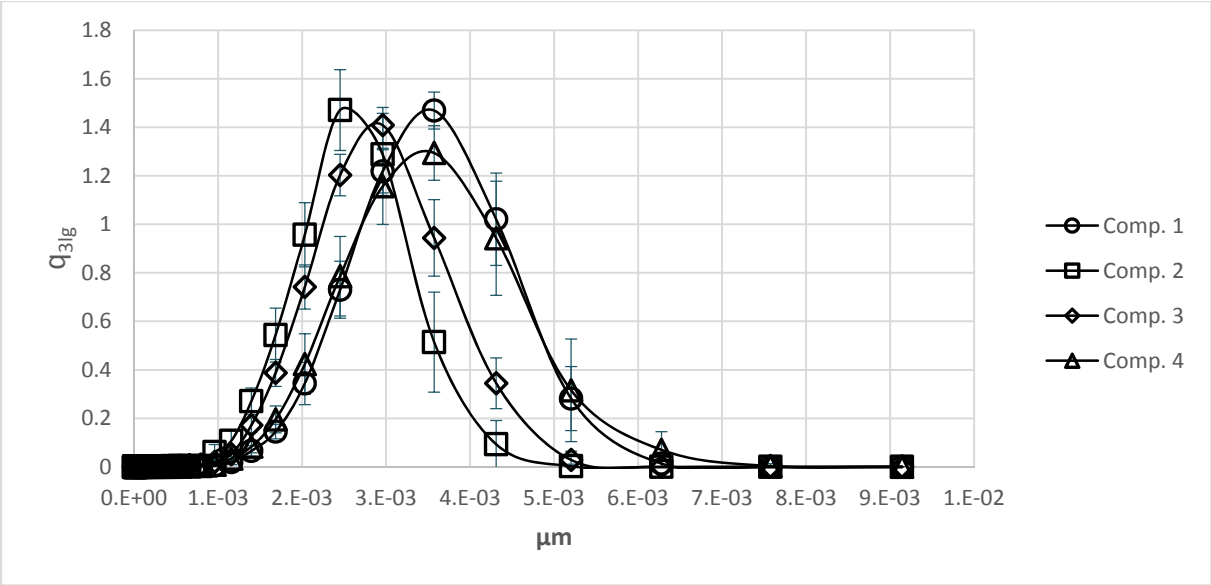

Figure 7. Granulation size distribution for the four compartmentalization's with breakage after 5 minutes.

The results show that the addition of breakage leads to a general decrease in the final particle sizes as expected. It looks like the inclusion of breakage counteracts the effect of the discretization leading to less distinction between the cases. When comparing the cases with and without breakage it is clear that the breakage effect is clearly biggest for Comp. 4 with a resolved impeller compartment. This shows the ability of the presented framework to isolate the effect of different mechanisms in different regions. Van den Dries et.al. [32] address the issue of granule homogeneity in relation to breakage. They show with a mechanistic model that there is a relation between granule breakage and homogeneity of the granules, where more breakage leads to more homogeneous granule compositions.

3.2 Temporal resolution

A further study was made to investigate the effects of particle property changes on the flow-field and especially on the changing flow field properties to the PBM solver, the distributions of: volume fraction, granular temperature, aggregation rates and shear rates. This was done via an analysis of the three CFD cases representing snapshot cases from a granulation, see Table 1.

Figure 8 shows the mass distribution of solid volume fractions of the granules averaged over the computational cell volumes. It shows that the flow model predicts a redistribution towards regions with lower solid volume fractions.

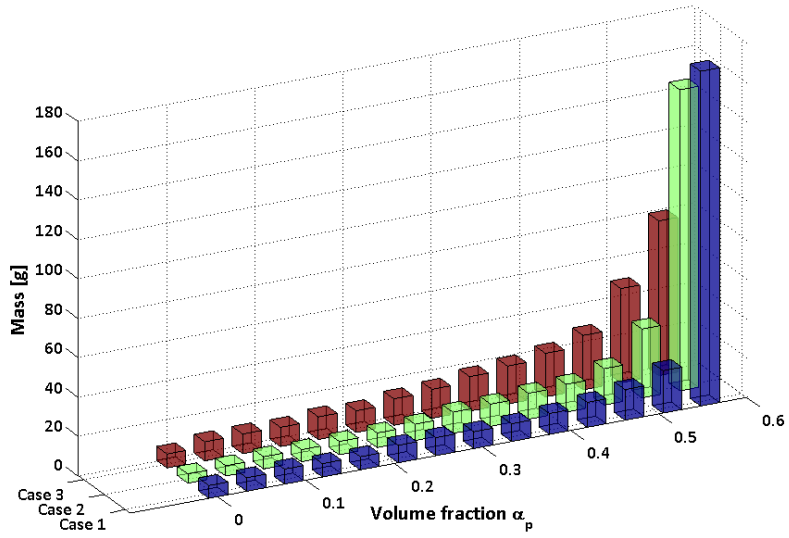

Figure 8.The mass distribution of solid volume fraction

This is coherent with the effect seen in Figure 9 of the mass distribution of granular temperature, where there is a tendency towards increasing granular temperatures for cases two and three. There is also a small peak at the high values of granular temperature and this peak can be located to the impeller region.

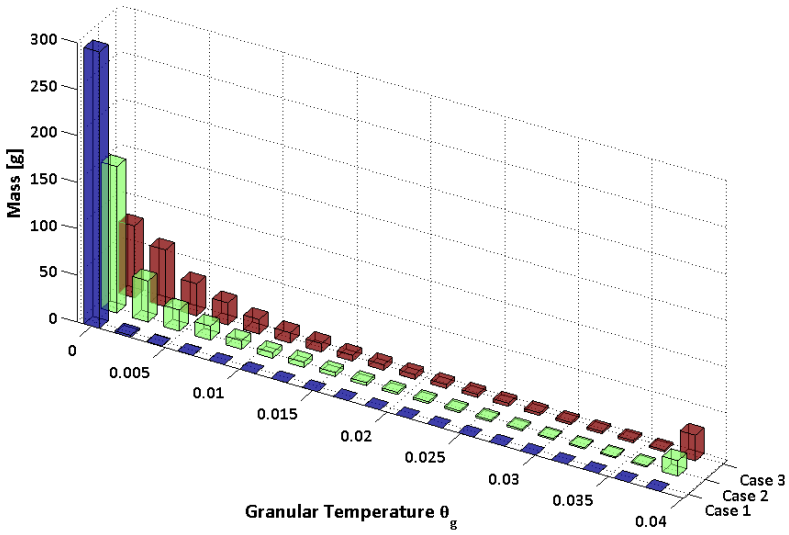

Figure 9. the mass distribution of granular temperature in [m^2/s^2].

In the impeller and bottom regions the strain rates are also at their peak and Figure 10 shows that there would be a trend towards lower strain rates as the granulation progresses affecting the breakage in the opposite way to the increase in granular temperatures. In order to determine the effect on the evolution of the breakage rate a more detailed mechanistic analysis would be needed.

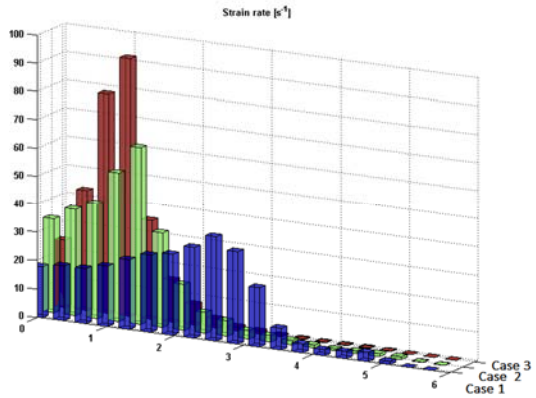

Figure 10. the mass distribution strain rates in [s^{-1}].

The distribution of the aggregation rate constant is shown in Figure 11.The aggregation rate is proportional to both the granular temperature and the solid volume fraction and their counteracting behaviors leads to the mass peak value being moved towards higher values. The effect of the impeller is stronger here since that area has retained high solid volume fraction with the increased granular temperature.

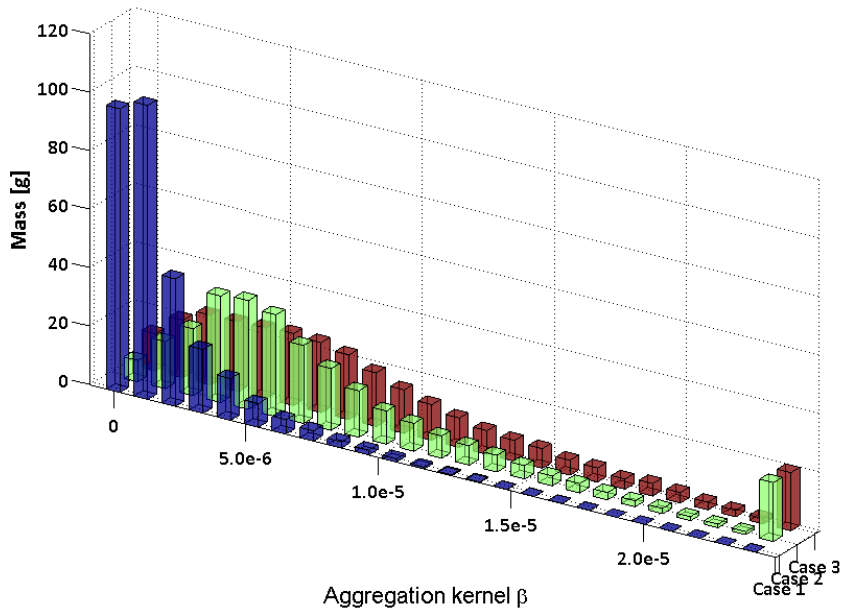

Figure 11. The mass distribution of the aggregation rate constant.

The averaged values of the aggregation rate constant can be found in Table 5. These values show a clear evolution from the first stages of granulation which could be captured by this type of meso-timescale analysis.

Table 5. Average aggregation rates for the three CFD cases, representing different time snapshots during a granulation.

Case	**1**	**2**	**3**
$\beta_0 \times 10^6$	0.65	3.12	3.06

From this information it is possible to just use a well-mixed one compartment model with a time dependent aggregation rate or to also use the spatial compartmentalization to update compartment shapes, sizes, interconnecting flow rates and internal properties during the progression of a granulation. For the simulations presented here the CFD relevant particle properties are estimated from literature experimental data. The aim would be to have PBM equations for the granule properties most relevant for the flow for example the frictional properties within the material and towards the walls. This would give a good resolution and understanding of the meso-scale processes. Further studies would be needed in order to determine the updating frequency of the flow field solution and the compartment structure. This would also require validation experiments, while this work aims to show that the solutions are affected by resolving meso-scale structures and providing a potential tool for analysis.

4. Conclusions

In this article we demonstrate a novel tool for analyzing meso-scales in high-shear granulation. From a CFD solution the flow conditions that the particles experience are extracted as distributions from which geometrical compartments are made. The inter-compartmental flow rates are calculated and the information is sent to a PBM solver to model evolution of particle properties. In an iterative process the information of the PBM solver, of particle property distributions can be sent back to the CFD solver to update the flow field and step by step reach the final product. The results show that the spatial compartmentalization is important leading to different final particle size distributions with the same mass volume weighted average of the included mechanisms. Analysis is needed of further process conditions and including more flow property dependent mechanisms like compaction and more elaborate breakage mechanisms. The temporal analysis shows that the model has potential to resolve meso-timescales and that it is possible to update compartment shapes, sizes, interconnecting flow rates and properties during the progression of a granulation.

Acknowledgements

AstraZeneca is greatly acknowledged for funding this project and for the cooperation. Professor Mike Hounslow, University of Sheffield, is acknowledged for helpful discussions in the initial phase of the project.

Appendix 1: Compartment data

The following tables A.1 to A.3 shows the compartments properties for the Comp. cases 1 – 3.

Table A.1. The properties inside the different compartments in CFD-case 2 and compartmentalization Comp. 1.

CFD-case 2 and compartmentalization Comp. 1				
Compartment	**Volume [m^3]**	**Volume fraction solid**	**β_0 [m/s]**	**S_0 [s^{-1}]**
1	0,000020	0,30	0	0
2	0,0016	0,26	5,0e-06	0

Table A.2. The properties inside the different compartments in CFD-case 2 and compartmentalization Comp. 2.

CFD-case 2 and compartmentalization Comp. 2				
Compartment	**Volume [m^3]**	**Volume fraction solid**	**β_0 [m/s]**	**S_0 [s^{-1}]**
1	0,000020	0,30	0	0
2	0,0039	0,26	2,1e-06	0

Table A.3. The properties inside the different compartments in CFD-case 2 and compartmentalization Comp. 3.

CFD-case 2 and compartmentalization Comp. 3				
Compartment	**Volume [m^3]**	**Volume fraction solid**	**β_0 [m/s]**	**S_0 [s^{-1}]**
1	2,0e-05	0,30	0	0
2	1,0e-03	0,34	5,0e-06	0
3	0,00056	0,11	5,1E-06	0

In Tables A.4 and A.5 the inter-compartmental fluxes for the compartment cases 1 to 3 are shown.

Table A.4. The inter-compartmental fluxes for the CFD-case 2 and compartmentalization Comp. 1 and 2.

Flow rates from CFD-case 2 and compartmentalization Comp. 1 and 2 [m3/s]				
Compartment	**1**	**2**	**-**	**-**
1	0	7,5e-03	-	-
2	7,5e-03	0	-	-
-	-	-	-	-
-	-	-	-	-

Table A.5. The inter-compartmental fluxes for the CFD-case 2 and compartmentalization Comp. 3.

Flow rates from CFD-case 2 and compartmentalization Comp. 3 [m3/s]				
Compartment	**1**	**2**	**3**	**-**
1	0	7,5e-03	0	-
2	7,5e-03	0	0,000948	-
3	0	0,00071	0	-
-	-	-	-	-

References

[1] A. Kumar, Gernaey, K. V. Gernaey, T. De Beer, I. Nopens, Model-based analysis of high shear wet granulation from batch to continuous processes in pharmaceutical production - A critical review, E. J. of Pharma. and Biopharma, vol. 85 Issue 3 (2013) pp. 814-832.

[2] S. M. Iveson, J. D. Litster, K. Hapgood, and B. J. Ennis, Nucleation, growth and breakage phenomena in agitated wet granulation processes: a review, *Powder Technol.*, vol. 117 no. 1–2 (2001) pp. 3–39.

[3] H. S. Tan, M. J. V. Goldschmidt, R. Boerefijn, M. J. Hounslow, a. D. Salman, and J. a. M. Kuipers, Building population balance model for fluidized bed melt granulation: lessons from kinetic theory of granular flow, *Powder Technol.* vol. 142 no. 2–3 (2004) pp. 103–109.

[4] M.J. Hounslow, The population balance as a tool for understanding particle rate processes Kona, pp. 179–193 (1998).

[5] R. Ramachandran, C. D. Immanuel, F. Stepanek, J. D. Litster, F. J. Doyle, A mechanistic model for granule breakage in population balances of granulation: theoretical kernel development and experimental validation. Chem. Eng. Research Design 87 (2009) 598-614.

[6] L. X. Liu, J. D. Litster, G. Associates, and H. H., Road, Coalescence of Deformable Granules in Wet Granulation Processes, AIChE J. vol. 46 no. 3 (2000) pp. 529–539.

[7] A. M. Nilpawar, G. K. Reynolds, A. D. Salman, and M. J. Hounslow, Surface velocity measurement in a high shear mixer, Chem. Eng. Sci. 61 (2006) pp. 4172 – 4178.

[8] J. A.Gantt, I. T. Cameron, J. D. Litster, E. P. Gatzke, Determination of coalescence kernels for high-shear granulation using DEM simulations, Powder Technol. vol. 170 no 2 (2006) pp. 53-63.

[9] A. Darelius, A. Rasmuson, B. van Wachem, I. Niklasson Björn, and S. Folestad, CFD simulation of the high shear mixing process using kinetic theory of granular flow and frictional stress models, Chem. Eng. Sci., vol. 63 no. 8 (2008) pp. 2188–2197.

[10] B. H. Ng, Y. L. Ding, and M. Ghadiri, Modelling of dense and complex granular flow in high shear mixer granulator—A CFD approach, Chem. Eng. Sci., vol. 64 no. 16 (2009) pp. 3622–3632.

[11] P. J. Abrahamsson, I. N. Björn, and a. Rasmuson, Parameter study of a kinetic-frictional continuum model of a disk impeller high-shear granulator, *Powder Technol.* vol. 238 (2013) pp. 20–26.

[12] P. J. Abrahamsson, S. Sasic and A. Rasmuson, On continuum modeling using kinetic-frictional models in high shear granulation. Particuology Vol. 13 (2014) p. 124-127.

[13] P. J. Abrahamsson, S. Sasic and A. Rasmuson, On the continuum modeling of dense granular flow in high shear granulation. Powder Technol. Vol. 268 (2014) p. 339-346.

[14] M. Khalilitehrani, P. J. Abrahamsson, and A. Rasmuson, The rheology of dense granular flows in a disc impeller high shear granulator, Powder Technol., vol. 249 (2013) pp. 309–315.

[15] M. Khaliliteherani, P. J. Abrahamsson, A. Rasmuson, Modeling dilute and dense granular flows in a high shear granulator, Powder Technol. Vol. 263 (2014) p. 45-49.

[16] M. Khaliliteherani, E. M. Gómez Fino, P. J. Abrahamsson, A. Rasmuson, Continuum modeling of multi-regime particle flows in high-shear mixing, Powder Technol. Vol. 280 (2015), p. 67-71.

[17] F. Bezzo, S. Macchietto, and C. C. Pantelides, General hybrid multizonal/CFD approach for bioreactor modeling, *AIChE J.* vol. 49 no. 8 (2003) pp. 2133–2148.

[18] I. Iliuta, A. Leclerc, and F. Larachi, Allothermal steam gasification of biomass in cyclic multi-compartment bubbling fluidized-bed gasifier/combustor - new reactor concept, *Bioresour. Technol.*, vol. 101 no. 9 (2010) pp. 3194–208.

[19 D. Guha, M. P. Dudukovic, P. A. Ramachandran, C. Reaction, and S. Louis, CFD-Based Compartmental Modeling of Single Phase Stirred-Tank Reactors, AIChE J. vol. 52, no. 5, (2006).

[20] A. H. Alexopoulos, P. Pladis, and C. Kiparissides, Nonhomogeneous Mixing Population Balance Model for the Prediction of Particle Size Distribution in Large Scale Emulsion Polymerization Reactors, Ind. Eng. Chem. Res. vol. 52 no. 35 (2013) pp. 12285–12296.

[21] Y. Le Moullec, C. Gentric, O. Potier, and J. P. Leclerc, Comparison of systemic, compartmental and CFD modelling approaches: Application to the simulation of a biological reactor of wastewater treatment, Chem. Eng. Sci. vol. 65 no. 1 (2010) pp. 343–350.

[22] M. Gresch, R. Brugger, A. Meyer, and W. Gujer, Compartmental Models for Continuous Flow Reactors Derived from CFD Simulations, Environ. Sci. Technol., vol. 43 no. 7 (2009) pp. 2381–2387.

[23] F. Bezzo and S. Macchietto, A general methodology for hybrid multizonal/CFD models Part I. Theoretical framework, Comput. Chem. Eng. vol. 28 no. 4 (2004) pp. 513–525.

[24] F. Bezzo and S. Macchietto, A general methodology for hybrid multizonal/CFD models Part II. Automatic zoning, Comput. Chem. Eng., vol. 28, no. 4 (2004) pp. 513–525.

[25] E. Kougoulos, a. G. Jones, and M. Wood-Kaczmar, CFD Modelling of Mixing and Heat Transfer in Batch Cooling Crystallizers, Chem. Eng. Res. Des. vol. 83, no. 1, (2005) pp. 30–39.

[26] S. K. Bermingham, H. J. M. Kramer, and G. M. van Rosmalen, Towards on-scale crystalliser design using compartmental models, Comput. Chem. Eng. vol. 22, (1998) pp. S355–S362.

[27] H. J. M. Kramer, J. W. Dijkstra, A. M. Neumann, R. Meadhra, and G. M. Van Rosmalen, Modelling of industrial crystallizers , a compartmental approach using a dynamic flow-sheeting tool, J. Crystal Growth vol. 166 (1996) pp. 1084–1088,.

[28] A. ten Cate, S. K. Bermingham, J. . Derksen, and H. J. M. Kramer, Compartmental modeling of an 1100L DTB crystallizer based on Large Eddy flow simulation, 10th Eur. Conf. Mix. (2000) pp. 255–264.

[29] X. Yu, An in-silico model of granulation, PhD thesis, University of Sheffield (2012).

[30] M. J. Hounslow, M. Oullion, G. K. Reynolds, Kinetic models for granule nucleation by the immersion mechanism." Powder Technol. vol. 189 no. 2 (2009) pp. 177-189.

[31] M. J. Hounslow, J. M. K. Pearson, T. Instone, Tracer studies of high-shear granulation: II. Population balance modeling, AIChE J. vol. 47 (2001) issue 9.

[32] K. van den Dries, O. M. de Vegt, V. Girard, H. Vromans, Granule breakage phenomena in a high shear mixer; influence of process and formulation variables and consequences on granule homogenity, Powder Technol. vol. 133 (2003) pp. 228–236.